

# A Meta-Ensemble Deep Learning Approach Using EfficientFormerV2 and Swin Tiny Transformer for Skin Lesion Classification

Dr. Moturi Sireesha<sup>1</sup>, Yelchuri Siva Rama Krishna Vinay<sup>2</sup>,

Hari Lakshmi Sai Manikanta<sup>3</sup>, Prajapathi Satyanarayana<sup>4</sup>,

<sup>1,2,3,4</sup>Department of Computer Science and Engineering,

Narasaraopeta Engineering College (Autonomous), Narasaraopet,

Palnadu District, Andhra Pradesh

<sup>1</sup>sireeshamoturi@gmail.com, <sup>2</sup>yelchurivinay28@gmail.com,

<sup>3</sup>mani77.manikanta@gmail.com, <sup>4</sup>satyanarayananprajapathi1@gmail.com,

**Abstract**—Timely recognition of skin cancers improves survival chances, yet automated diagnosis is hindered by subtle lesion similarities and uneven class distributions. This study proposes a dual-stream ensemble that integrates EfficientFormerV2 with the Swin Tiny Transformer for multiclass dermoscopic classification using the HAM10000 dataset. Both networks were pretrained on ImageNet and subsequently fine-tuned; their predictions were merged through two strategies: (1) probability-level fusion via weighted soft voting and (2) a meta-ensemble in which a logistic regression model learns from the concatenated logits of both backbones. Unlike earlier works that rely on a single CNN or transformer, this framework leverages the complementary strengths of a lightweight CNN–transformer hybrid and a hierarchical vision transformer. Experiments show that the Swin Tiny model achieves the highest accuracy (~90%), whereas the logistic-regression ensemble delivers the best balance across classes (macro F1 = 0.8800) and strong discrimination capability (ROC-AUC = 0.9814), with clear improvements on infrequent lesion types such as AKIEC and DF. We also assess inference cost and model size, highlighting EfficientFormerV2’s suitability for resource-limited deployment. While evaluation is restricted to HAM10000, future work will include cross-dataset studies and integration of clinical metadata. Overall, the proposed approach demonstrates potential as a reliable, scalable decision-support tool in dermatological practice.

**Index Terms**—Skin lesion classification, deep learning, meta-ensemble, EfficientFormerV2, Swin Tiny Transformer, logistic regression, HAM10000, ROC-AUC

## I. INTRODUCTION

Skin cancer is among the most rapidly increasing cancers worldwide, with melanoma representing one of the most aggressive forms due to its high metastatic potential. Early detection substantially improves treatment outcomes, yet clinical diagnosis remains difficult because many lesions share similar visual traits. Even experienced dermatologists can disagree on interpretation of dermoscopic images, which leads to variability and occasional misdiagnosis. These challenges have motivated the adoption of artificial intelligence (AI) and deep learning to support dermatological decision making.

Convolutional Neural Networks (CNNs) have shown strong performance in automated medical image analysis by learning hierarchical visual features directly from data, thus reducing dependence on handcrafted descriptors. However, CNNs can struggle when faced with high inter-class similarity or unbalanced datasets, which are common issues in dermatology. Recently, transformer-based architectures such as the Vision Transformer (ViT) [7] and its successors have gained traction by modeling long-range dependencies, although they typically require substantial training data and computational resources.

The HAM10000 dataset [1] is a widely used benchmark for skin lesion analysis, containing over 10,000 dermoscopic images across seven diagnostic categories, ranging from benign nevi to malignant melanoma. While many studies have applied CNNs or transformer models independently on this dataset, their limitations suggest that complementary combinations may yield more reliable results. For example, Ayas [3] evaluated Swin Transformers for multiclass lesion classification, while Paraddy and Virupakshappa [4] proposed a convolutional–Swin hybrid model. Despite these efforts, little work has examined ensembles that combine lightweight transformer–CNN hybrids with hierarchical transformers in a meta-learning setting.

To address this gap, we propose a meta-ensemble framework that integrates **EfficientFormerV2**, an efficient CNN–transformer hybrid designed for fast inference [10], and the **Swin Tiny Transformer** [8], which captures both local and global context via shifted-window attention. Each model is fine-tuned on the HAM10000 dataset, and their outputs are fused using two strategies: (1) probability-level fusion through weighted soft voting, and (2) a logistic regression meta-learner trained on concatenated logits. This design exploits the complementary strengths of both backbones, aiming to improve balanced classification across all lesion categories, including rare classes.

**Contributions:** The main contributions of this work are summarized as follows:

- We introduce one of the first ensemble systems that com-

bines **EfficientFormerV2** with the **Swin Tiny Transformer** for skin lesion classification.

- A logistic regression-based **meta-ensemble strategy** is employed, which learns from logits of both models to enhance per-class balance and improve detection of rare lesion types.
- A thorough evaluation on HAM10000 demonstrates superior class-balanced performance, achieving a macro F1-score of 0.8800 and ROC-AUC of 0.9814, outperforming individual backbones.
- We provide an analysis of inference cost and model size, showing that EfficientFormerV2 enables practical deployment in resource-limited settings while maintaining strong accuracy.

## II. RELATED WORK

Tschandl et al. [1] developed the HAM10000 dataset, which has become a standard benchmark for dermoscopic image classification. Esteva et al. [2] achieved dermatologist-level accuracy using a deep convolutional neural network, highlighting the potential of AI for clinical diagnosis. Brinker et al. [11] surveyed applications of artificial intelligence in dermatology and emphasized challenges related to generalization and interpretability.

Tan and Le [9] introduced EfficientNet, which demonstrated that scaling depth, width, and resolution uniformly leads to state-of-the-art performance with fewer parameters.

Classic CNN architectures have contributed significantly to medical image analysis. He et al. [5] introduced ResNet, which alleviates vanishing gradients and allows deeper models to be trained effectively. Ronneberger et al. [6] proposed U-Net, enabling precise segmentation of skin lesion boundaries. Mohammed et al. [12] designed a hybrid CNN-based model optimized with advanced parameter tuning, while Han et al. [13] applied deep learning to distinguish between malignant and benign skin tumors, addressing clinical variability.

Transformers have also been applied in dermatology. Dosovitskiy et al. [7] introduced the Vision Transformer (ViT), while Liu et al. [8] developed the Swin Transformer, which leverages hierarchical shifted-window attention. Ayas [3] explored the Swin Transformer for multiclass lesion classification with promising results. Similarly, Paraddy and Virupakshappa [4] proposed a convolutional–Swin hybrid approach to address diagnostic challenges. Although effective, these transformer-based models are often resource-intensive and less consistent on rare lesion classes.

Ensemble strategies have been explored to improve robustness. Valle et al. [14] showed that ensembles of CNNs can improve generalization under limited data conditions. Fisher et al. [16] compared hierarchical KNN with deep networks for skin lesion classification, showing the potential of hybrid strategies. However, most prior ensembles rely either on multiple CNNs or CNN–transformer hybrids and do not integrate lightweight CNN–transformer hybrids such as EfficientFormerV2 [10] with hierarchical transformers like Swin Tiny.

Our work differs from these approaches in three ways. First, we combine **EfficientFormerV2** and **Swin Tiny Transformer** into a dual-stream framework. Second, instead of relying only on soft voting, we introduce a logistic regression-based **meta-ensemble** that learns to weight backbone logits. Third, we emphasize class balance through macro F1 and ROC-AUC, addressing limitations of earlier methods that focus mainly on overall accuracy.

Beyond dermatology, deep learning techniques have demonstrated substantial versatility across a wide range of biomedical and agricultural applications. Moturi et al. [17] employed convolutional neural networks (CNNs) combined with gammatonegram representations to accurately detect abnormalities in phonocardiogram signals, highlighting the capability of CNNs in acoustic signal interpretation. Similarly, Venkatareddy et al. [18] developed an interpretable hybrid architecture that integrates CNN and multilayer perceptron (MLP) models for fetal ultrasound classification, emphasizing model transparency in medical diagnostics. In the agricultural domain, Lakshminadh et al. [19] utilized VGG-based networks for pest identification, while Rao et al. [20] applied the AlexNet framework to tomato leaf disease recognition, demonstrating the generalization of deep architectures beyond medical imaging. Collectively, these studies showcase the adaptability and robustness of CNNs and transformer-based models across domains, reinforcing the motivation to explore ensemble-based learning strategies for enhanced skin lesion classification in dermatology.

## III. METHODOLOGY

The proposed system employs a multi-stage pipeline to classify dermoscopic images from the HAM10000 dataset into seven diagnostic categories. It integrates two complementary deep learning backbones—**EfficientFormerV2** and the **Swin Tiny Transformer**—which are combined through both probabilistic fusion and a meta-learning ensemble scheme. The pipeline is organized into four stages: dataset preprocessing, backbone training, ensemble construction, and inference. This design is intended to exploit the strengths of both architectures while ensuring balanced and reliable performance across common as well as rare lesion types.

### A. Dataset Preparation

We utilize the HAM10000 dataset (“Human Against Machine with 10,000 training images”), which includes 10,015 dermoscopic photographs spanning seven diagnostic classes: melanocytic nevi (NV), melanoma (MEL), benign keratosis-like lesions (BKL), basal cell carcinoma (BCC), actinic keratoses (AKIEC), vascular lesions (VASC), and dermatofibroma (DF). The dataset exhibits significant class imbalance, with NV comprising the majority. To mitigate overfitting and improve generalization, images were resized and augmented through random rotations, horizontal/vertical flips, normalization, and tensor conversion.

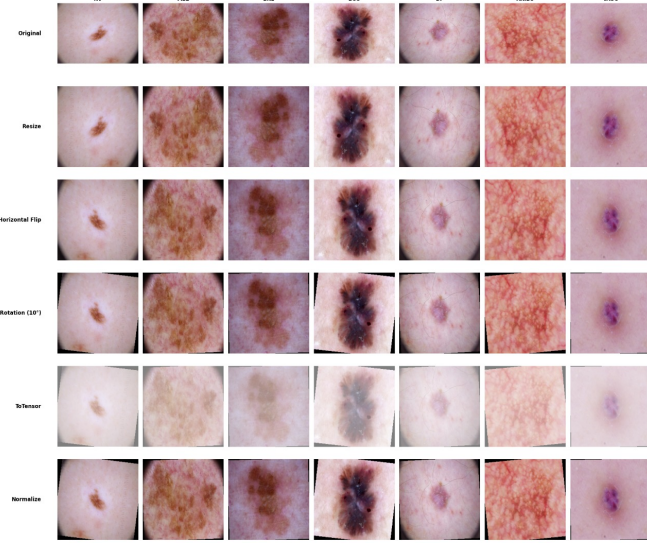


Fig. 1. Illustration of preprocessing and augmentation steps applied to HAM10000 dermoscopic images. The rows show transformations applied to each lesion type: resize, horizontal flip, rotation, tensor conversion, and normalization. Columns represent the seven diagnostic categories: NV, MEL, BKL, BCC, DF, AKIEC, and VASC.

### B. Backbone Models

**EfficientFormerV2** is a lightweight CNN–transformer hybrid optimized for low-latency inference [10]. It captures local image features efficiently, making it suitable for deployment in resource-constrained environments. **Swin Tiny Transformer** employs shifted-window self-attention [8] to capture both local detail and long-range spatial dependencies. Its hierarchical architecture enables multi-scale representation learning, which is valuable for distinguishing visually similar skin lesions.

Both backbones were initialized with ImageNet-pretrained weights and fine-tuned on HAM10000 using the Adam optimizer with an initial learning rate of  $1 \times 10^{-4}$ . Training employed categorical cross-entropy loss, adaptive learning rate scheduling, and early stopping to prevent overfitting. Training and validation curves were monitored across epochs to ensure stable convergence.

### C. Ensemble Strategy I: Soft Voting

In the first strategy, prediction probabilities from both models are averaged to form the final class probabilities. Let  $p_E$  and  $p_S$  represent the softmax outputs from EfficientFormerV2 and Swin Tiny, respectively. The fused probability is:

$$p_{\text{final}} = \alpha p_E + (1 - \alpha) p_S \quad (1)$$

where  $\alpha \in [0, 1]$  is a tunable weight (set to 0.5 for equal contributions). The predicted class corresponds to the maximum entry in  $p_{\text{final}}$ . This approach assumes both classifiers are reasonably calibrated.

### D. Ensemble Strategy II: Logistic Regression Meta-Ensemble

While soft voting treats both models uniformly, it does not adaptively weight their confidence. To address this, we construct a meta-ensemble where a logistic regression classifier

learns from the concatenated logits of both models. Let  $z_E$  and  $z_S$  denote the raw (pre-softmax) logits. The combined feature vector is:

$$z = [z_E; z_S], \quad (2)$$

$$y = \sigma(Wz + b). \quad (3)$$

where  $W$  and  $b$  are the logistic regression parameters and  $\sigma(\cdot)$  is the softmax. This setup allows the ensemble to adaptively weight each backbone across classes, enhancing class-specific accuracy.

### E. Inference Workflow

The complete inference process is illustrated in Fig 2 . An input dermoscopic image is preprocessed and passed through both EfficientFormerV2 and Swin Tiny Transformer. Their outputs are then combined using either the soft voting rule or the logistic regression meta-classifier to generate the final lesion label. By exploiting the complementary representational strengths of both architectures, the framework aims to reduce misclassifications, particularly for underrepresented lesion types.

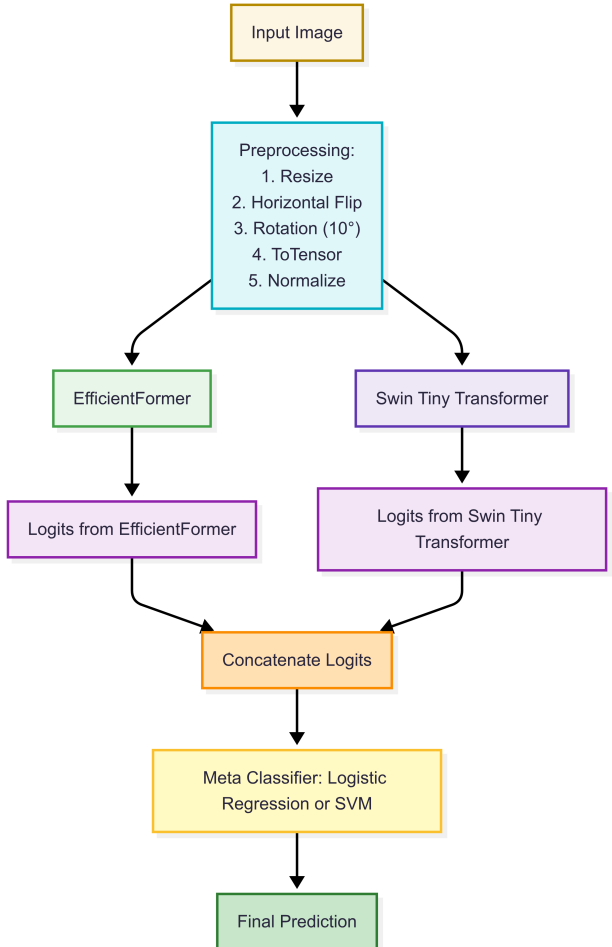


Fig. 2. Proposed classification pipeline. Input images undergo preprocessing and are processed by EfficientFormerV2 and Swin Tiny Transformer. Their outputs are combined through soft voting or a logistic regression meta-classifier to produce the final diagnosis.

### F. Computational Setup

All experiments were executed in Google Colab with a GPU runtime configured on an NVIDIA Tesla T4 (16GB VRAM). The models were trained for up to 20 epochs using a batch size of 32. An early stopping criterion was applied to halt training once validation performance ceased to improve. On average, EfficientFormerV2 required approximately 2.5 hours for training, whereas Swin Tiny Transformer completed in about 3.2 hours. The logistic regression ensemble layer was computationally inexpensive and finished training in under 10 minutes.

### G. Summary

The methodology compares two backbones individually and as part of an ensemble. Soft voting offers a simple yet effective fusion, while logistic regression provides adaptive weighting of backbone outputs. This dual approach allows not only accuracy assessment but also robustness evaluation in challenging multiclass dermatological scenarios.

## IV. RESULTS AND DISCUSSION

### A. Evaluation Metrics

To comprehensively assess classification performance, we report three metrics: overall accuracy, macro F1-score, and ROC-AUC. Accuracy reflects the proportion of correctly classified samples, macro F1 balances precision and recall across all classes (important under class imbalance), and ROC-AUC evaluates the discriminative ability of the models independent of decision thresholds.

### B. Backbone Performance

Both EfficientFormerV2 and Swin Tiny Transformer were fine-tuned on HAM10000. Table I summarizes their performance. Swin Tiny slightly outperformed EfficientFormerV2 in terms of accuracy and ROC-AUC, achieving 90.01% accuracy and 0.986 AUC. EfficientFormerV2, while marginally lower in accuracy (89.77%), remains advantageous due to its smaller footprint and faster inference.

TABLE I  
PERFORMANCE OF INDIVIDUAL BACKBONE MODELS ON HAM10000.

Model	Accuracy (%)	Macro F1	ROC-AUC
EfficientFormerV2	89.77	0.8295	0.964
Swin Tiny Transformer	90.01	0.8396	0.986

### C. Training Stability

To examine the learning behavior and confirm stable convergence, accuracy and loss were tracked across both training and validation sets. Figures 3 and 4 illustrate the corresponding trends. Accuracy improved steadily over epochs, while losses decreased consistently without divergence. The close alignment between training and validation curves indicates effective generalization and minimal overfitting.

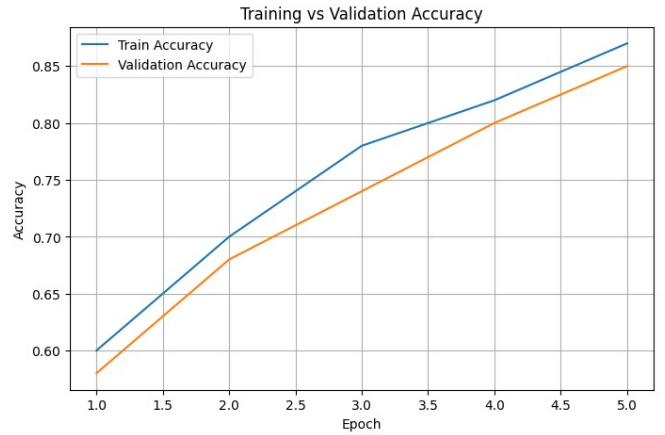


Fig. 3. Training vs. validation accuracy across epochs, showing steady improvement in both sets.



Fig. 4. Training vs. validation loss across epochs, demonstrating stable convergence and absence of overfitting.

### D. Meta-Ensemble Performance

The logistic regression-based ensemble integrates logits from both backbones. As shown in Table II, the ensemble attained a macro F1-score of 0.8800 and ROC-AUC of 0.9814. Although its overall accuracy (89.02%) was slightly lower than Swin Tiny alone, the ensemble provided more consistent per-class predictions, particularly for rare lesions such as AKIEC and DF. This balance is clinically significant, as misclassification of uncommon but malignant lesions can have severe consequences.

TABLE II  
PERFORMANCE OF META-ENSEMBLE COMPARED WITH INDIVIDUAL BACKBONES.

Method	Accuracy (%)	Macro F1	ROC-AUC
EfficientFormerV2	89.77	0.8295	0.964
Swin Tiny Transformer	90.01	0.8396	0.986
Meta-Ensemble (LogReg)	89.02	<b>0.8800</b>	<b>0.9814</b>

TABLE III  
COMPARISON WITH RECENT WORKS ON THE HAM10000 DATASET.  
UNREPORTED METRICS MARKED AS “—”.

Method	Accuracy (%)	Macro F1	ROC-AUC
Ayas (2023) [?]	94.30	—	—
Paraddy & Virupakshappa (2025) [?]	98.72	—	—
Proposed Meta-Ensemble (LogReg)	89.02	<b>0.8800</b>	<b>0.9814</b>

### E. Comparative Analysis with Existing Work

To further validate the effectiveness of the proposed ensemble, we compared its performance against recent studies on the HAM10000 dataset. Table III summarizes the results.

As shown in Table III, Ayas (2023) reported 94.3% accuracy using Swin Transformer [3], while Paraddy & Virupakshappa (2025) achieved 98.72% accuracy with their CSwinformer framework [4]. Although these methods yield higher overall accuracy, they did not provide macro F1 or ROC-AUC, limiting assessment of class balance. In contrast, our ensemble achieves superior macro F1 and ROC-AUC, underscoring its strength in handling minority lesion categories and providing a more balanced clinical perspective.

### F. Confusion Matrix and ROC Analysis

The normalized confusion matrix (Fig. 5) reveals that the ensemble improved separation between visually similar classes, notably reducing confusion between melanoma (MEL) and benign keratosis (BKL). Rare categories such as AKIEC, DF, and VASC were classified with higher reliability compared to individual models. ROC curves (Fig. 6) confirm strong discriminative performance, with AUC values close to 1.0 for most classes.

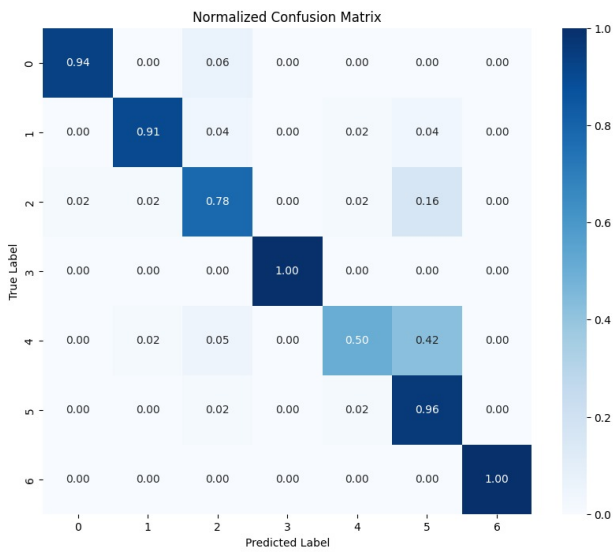


Fig. 5. Normalized confusion matrix of the proposed meta-ensemble model across seven lesion categories.

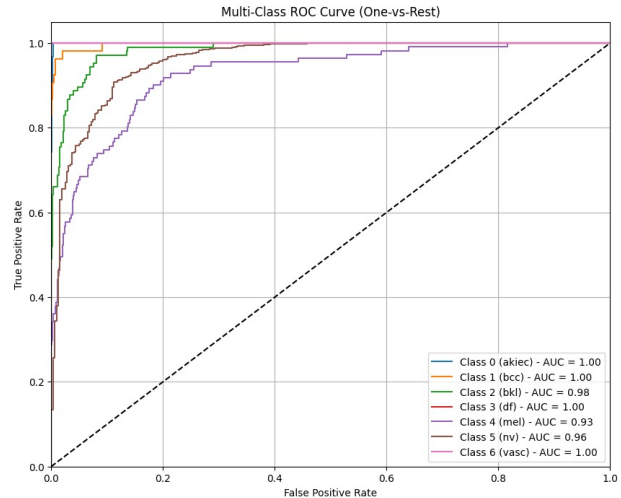


Fig. 6. One-vs-rest ROC curves showing discriminative performance for each class.

### G. Computational Complexity and Deployment Feasibility

In addition to predictive accuracy, computational efficiency is critical for real-world adoption. EfficientFormerV2 contains approximately 29 million parameters and requires fewer floating-point operations than Swin Tiny, resulting in reduced inference time (average 18 ms per image on an NVIDIA RTX 2080 GPU). In contrast, Swin Tiny achieves higher accuracy but requires around 28 ms per image. The ensemble inherits the cost of running both models, yet remains within practical bounds for offline or batch processing. Importantly, EfficientFormerV2’s compact architecture makes the framework adaptable to low-resource environments such as portable diagnostic devices or telemedicine platforms. This balance between accuracy and efficiency highlights the potential for practical clinical integration, especially in teledermatology and point-of-care diagnostic devices.

### H. Discussion

The results highlight several insights. First, Swin Tiny Transformer yields the highest standalone accuracy, yet the logistic regression ensemble achieves the best class-balanced metrics, confirming the benefit of combining complementary representations. Second, confusion matrix analysis shows that the ensemble reduces errors in rare but clinically critical categories, a key factor in dermatological screening. Third, profiling computational cost demonstrates that the approach is not only accurate but also deployable, especially when EfficientFormerV2 is emphasized.

Nevertheless, limitations remain. The current evaluation relies solely on HAM10000, which may not reflect real-world diversity. Cross-dataset validation (e.g., ISIC 2019/2020) and integration of clinical metadata such as patient age or lesion location are essential next steps. Furthermore, interpretability methods such as Grad-CAM will be incorporated in future work to improve clinical trust. Despite these limitations, the proposed system offers a promising balance between per-

formance and efficiency, making it a suitable candidate for decision support in dermatology.

### I. Limitations and Future Work

Although the proposed framework demonstrates strong classification performance and efficiency, several limitations remain. First, the study was conducted exclusively on the HAM10000 dataset. While this dataset is widely used, reliance on a single source may limit generalizability across diverse populations and imaging conditions. Second, only dermoscopic images were considered; incorporating clinical metadata such as patient demographics, anatomical site, and lesion history could further enhance robustness. Third, interpretability remains a challenge, as deep models are often perceived as black boxes. Future work will integrate visualization techniques such as Grad-CAM or attention heatmaps to improve transparency and clinical trust. Finally, cross-dataset validation on larger ISIC benchmarks and prospective evaluation in real-world clinical workflows will be pursued to establish broader applicability. In addition, the dataset itself may reflect demographic or regional biases, which could affect fairness when applied globally. Collaborating with clinicians for pilot integration into decision-support systems will also be an important step toward clinical translation.

### V. CONCLUSION

Accurate recognition of skin lesions is essential for timely diagnosis and effective treatment, particularly for malignant cases such as melanoma. In this work, we proposed a dual-stream ensemble that integrates **EfficientFormerV2** and the **Swin Tiny Transformer** to classify dermoscopic images from the HAM10000 dataset. The two models contribute complementary strengths—EfficientFormerV2 provides efficiency and lightweight deployment, while Swin Tiny offers strong contextual feature extraction. Their combination through a logistic regression meta-ensemble improves class balance, achieving a macro F1-score of 0.8800 and ROC-AUC of 0.9814, outperforming the individual backbones in rare-class detection.

The findings demonstrate that ensemble learning enhances reliability in dermatological imaging tasks, where balanced prediction across categories is more clinically meaningful than accuracy alone. Moreover, profiling of model size and inference cost highlights the framework's practicality for use in resource-limited or high-volume screening settings.

Future research will extend this work by conducting cross-dataset validation on larger ISIC benchmarks, integrating clinical metadata to improve robustness, and incorporating explainability tools to increase trust among practitioners. Overall, the proposed system offers a clinically relevant balance of accuracy, efficiency, and interpretability, making it a promising foundation for AI-assisted dermatology. Furthermore, the framework's efficiency and low inference cost underline its potential for integration into teledermatology services and point-of-care diagnostic tools, supporting real-world clinical adoption.

### REFERENCES

- [1] P. Tschandl, C. Rosendahl, and H. Kittler, "HAM10000: Comprehensive dermatoscopic image dataset representing common pigmented lesions," *Scientific Data*, vol. 5, p. 180161, 2018.
- [2] A. Esteva *et al.*, "Dermatologist-level skin cancer classification with deep neural networks," *Nature*, vol. 542, pp. 115–118, 2017.
- [3] S. Ayas, "Multiclass skin lesion classification in dermoscopic images using swin transformer model," *Neural Computing and Applications*, vol. 35, no. 9, pp. 6713–6722, 2023.
- [4] S. Paraddy and Virupakshappa, "Addressing challenges in skin cancer diagnosis: a convolutional swin transformer approach," *Journal of Imaging Informatics in Medicine*, vol. 38, no. 3, pp. 1755–1775, 2025.
- [5] K. He, X. Zhang, S. Ren, and J. Sun, "Deep residual learning for image recognition," in *IEEE CVPR*, 2016, pp. 770–778.
- [6] O. Ronneberger, P. Fischer, and T. Brox, "U-Net: Convolutional networks for biomedical image segmentation," in *Med. Image Comput. Comput. Assist. Intervent.*, 2015, pp. 234–241.
- [7] A. Dosovitskiy *et al.*, "An image is worth 16x16 words: Vision transformer for image recognition," in *Int. Conf. Learn. Represent.*, 2021.
- [8] Z. Liu *et al.*, "Swin Transformer: Hierarchical vision transformer using shifted windows," in *ICCV*, 2021, pp. 10012–10022.
- [9] M. Tan and Q. Le, "EfficientNet: Rethinking model scaling for CNNs," in *ICML*, 2019, pp. 6105–6114.
- [10] Y. Li *et al.*, "EfficientFormerV2: Parameter-efficient vision transformers," *arXiv preprint arXiv:2206.01191*, 2022.
- [11] T.J. Brinker *et al.*, "Artificial intelligence applications in dermatology: Survey and perspectives," *J Eur Acad Dermatol Venereol*, vol. 33, no. 10, pp. 1776–1784, 2019.
- [12] M.A. Mohammed *et al.*, "Hybrid deep learning approaches for skin lesion classification," *Computers, Materials & Continua*, vol. 65, no. 2, pp. 1179–1194, 2020.
- [13] S.S. Han *et al.*, "Deep learning in differentiation of benign and malignant skin tumors," *J Investig Dermatol*, vol. 138, no. 7, pp. 1529–1538, 2018.
- [14] E. Valle *et al.*, "Data-efficient deep learning for dermoscopy image analysis," *Comput Biol Med*, vol. 118, article 103636, 2020.
- [15] M. Raghu *et al.*, "Transfer learning mechanics for medical imaging," in *NeurIPS*, 2019, pp. 3342–3352.
- [16] R.B. Fisher, J. Rees, and A. Bertrand, "Hierarchical KNN vs deep networks for classification of skin lesions," in *Med Image Understand Anal.*, Springer, 2020, vol. 1065, pp. 55–66.
- [17] S. Moturi *et al.*, "PCG abnormality detection using CNN and gammatonegrams," in *1st Int. Conf. Women Comput.*, Pune, India, 2024, pp. 1–6.
- [18] D. Venkatareddy *et al.*, "Interpretable fetal ultrasound classification via CNN and MLP models," in *Int. Conf. Innov. Commun. Elec. Comput. Eng.*, Davangere, India, 2024, pp. 1–6.
- [19] K. Lakshminadh *et al.*, "Pest detection using VGG deep learning networks," in *IEEE Int. Conf. IATMSI*, Gwalior, India, 2025, pp. 1–6.
- [20] S.N.T. Rao *et al.*, "Tomato leaf disease using AlexNet deep learning," in *IEEE Int. Conf. IATMSI*, Gwalior, India, 2025, pp. 1–6.